Cytometry
PART A
Journal of the International Society for Advancement of Cytometry

Detection of Pathogenic *E. coli* O157:H7 by a Hybrid Microfluidic SPR and Molecular Imaging Cytometry Device

Michael D. Zordan,[1,2,3] Meggie M. G. Grafton,[1,2,3] Ghanashyam Acharya,[1,3] Lisa M. Reece,[2,3,4] Christy L. Cooper,[2,3,4] Arthur I. Aronson,[5] Kinam Park,[1,6] James F. Leary[1,2,3,4]*

[1]Weldon School of Biomedical Engineering, Purdue University, West Lafayette, Indiana

[2]Bindley Bioscience Center, Purdue University, West Lafayette, Indiana

[3]Birck Nanotechnology Center, Purdue University, West Lafayette, Indiana

[4]Department of Basic Medical Science, School of Veterinary Medicine, Purdue University, West Lafayette, Indiana

[5]Department of Biological Sciences, Purdue University, West Lafayette, Indiana

[6]Department of Industrial and Physical Pharmacy, Purdue University, West Lafayette, Indiana

Received 15 August 2008; Revision Received 31 October 2008; Accepted 5 November 2008

Additional Supporting Information may be found in the online version of this article.

Grant sponsor: USDA (through the Center for Food Safety Engineering at Purdue University); Grant number: 102145

*Correspondence to: James F. Leary, Birck Nanotechnology Center, Purdue University, Room 2021, 1205 W. State Street, West Lafayette, IN 47907, USA

Email: jfleary@purdue.edu

Published online 00 Month 2008 in Wiley InterScience (www.interscience.wiley.com)

DOI: 10.1002/cyto.a.20692

ISAC
International Society for Advancement of Cytometry

Abstract

Current methods to screen for bacterial contamination involve using costly reagents such as antibodies or PCR reagents or time-costly growth in cultures. There is need for portable, real-time, multiplex pathogen detection technology that can predict the safety of food. Surface plasmon resonance (SPR) imaging is a sensitive, label-free method that can detect the binding of an analyte to a surface by the changes in refractive index that occur upon binding. We have designed a hybrid microfluidic biochip to perform multiplexed detection of single-celled pathogens using a combination of SPR and fluorescence imaging. The device consists of an array of gold spots, each functionalized with a capture biomolecule targeting a specific pathogen. This biosensor array is enclosed by a polydimethylsiloxane microfluidic flow chamber that delivers a magnetically concentrated sample to be tested. The sample is imaged by SPR on the bottom of the biochip and epi-fluorescence on the top. The prototype instrument was successfully able to image antibody-captured *E. coli* O157:H7 bacteria by SPR and fluorescence imaging. The efficiency of capture of these bacteria by the magnetic particles was determined using spectrophotometric ferric oxide absorbance measurements. The binding of the *E. coli* to each spot was quantified by measuring the percent of the gold spot area upon which the bacteria was bound and analyzed using NIH ImageJ software. This hybrid imaging approach of pathogenic *E. coli* detection coupled with an estimate of relative infectivity is shown to be a working example of a testing device for potential foodborne pathogens.

Key terms

foodborne pathogens; microbes; detection; microfluidic; cytometry; imaging; surface plasmon resonance; *E. coli* O157:H7

THE increased incidence of fatal pathogen-contaminated food supplies places a new emphasis on the rapid detection and quantification of the foodborne pathogens. This issue has been further compounded by the fact that many high-risk foodborne pathogens are easily transmitted through food supplies, thus constituting a major public health problem. Accurate and rapid identification of pathogens in food is to facilitate timely and appropriate actions in the event of a contamination. Conventional pathogen detection methods involve enriching the sample and performing various media-based metabolic tests (1). These detection methods are elaborate and typically require 2–7 days to obtain results. Detection using magnetic beads coated with pathogen-specific antibodies or enzyme-linked immunosorbent assays still require several hours for completing the tests (2,3). The oligonucleotide array method based on amplification and hybridization of DNA fragments of pathogenic bacteria also takes more than several hours (4). Some techniques also require rather expensive special instruments, such as flow cytometry (5) and real-time PCR (6). Hence, a rapid, label-free, and easy-to-use biosensor capable of detecting toxigenic bacteria in a few minutes is of immediate importance.

The ability to screen for multiple pathogens in one assay is of great importance. It is possible to accomplish this using an array of immobilized capture biomolecules. In this setup, the pathogen will bind to and be captured at a specific spatial position in the array, corresponding to the appropriate capture molecule. There are many types of biomolecules that can be used to specifically bind pathogens, such as antibodies, short peptides, and aptamers. Further, the capture biomolecules can be spotted on a surface in a spatially separated array that will allow for the simultaneous multiplex detection of different pathogens in the same sample. Biosensor arrays such as these have been demonstrated using peptides (7), aptamers (8), and antibodies (9). In addition, surface plasmon resonance (SPR) imaging has been used previously to measure simultaneous binding events on microarrays (9–12). Additionally, surface-based detection requires lower quantities of the costly capture biomolecules than bulk methods.

Basic Principles of Surface Plasmon Resonance Imaging

SPR imaging can detect the presence of molecules or cells or pathogens bound to the biosensor surface by measuring the changes in the local refractive indices (13,14). SPR imaging involves the measurement of the intensity of light reflected at a dielectric covered by a metal (e.g., gold) layer of ~50 nm thickness. The charge-density propagating along the interface of the thin metal layer and the dielectric is composed of surface plasmons. These surface plasmons are excited by an evanescent field typically generated by total internal reflection via a prism coupler. The wave vector of the surface plasmons is dependent upon the properties of the prism, the gold layer, and the surrounding dielectric medium (glass slide) (15). Under appropriate conditions, the free electrons come in resonance with the incident light and a surface plasmon is generated. At this resonance condition, the reflection decreases sharply to a minimum because incident photons will induce surface plasmons instead of being reflected. Changes in dielectric properties, e.g., thickness or refractive index, of the surrounding medium lead to changes in the wave vector and consequently there is a shift of plasmon resonance minimum of the reflected light (15).

The binding of biomolecules or bacteria to the surface is sensitively detected, as the plasmon resonance is extremely sensitive to surface dielectric properties and the fact that resonance occurs only in a small range of conditions including refractive index, wavelength, and angle of incidence (10,15,16). Resonance angle measurements have been used for chemical and biochemical sensing (16). Only p-polarized light in plane of incidence with the electric field vector oscillating in the plane of the metal film is able to couple to the plasmon mode. The s-polarized light, with its electric field vector oriented perpendicular to the metal film, does not excite plasmons but is reflected by the metal surface and can be used as a reference signal to improve the sensitivity (17,18). Thus, in SPR imaging, the reflectivity change resulting from biomolecular and cellular binding on the biosensor surface is measured before and after analyte binding.

Molecular Imaging to Provide Additional "Pathogen State" Information

In some instances, it is also important to not only detect the presence of pathogens by SPR but also the state of the pathogen. For example, the presence of pathogenic bacteria is a useful information, but that information would be of much greater use if we also obtain a measure of the "pathogen state." For this reason, simultaneous fluorescence molecular imaging contained in a hybrid SPR/molecular imaging device is significantly more powerful. The pathogen state information can extend from simple viability measures to fluorescent molecular probes of metabolic or functional capabilities of the detected pathogen (19–22). This "functional" information may prove more valuable when combined with structural information. This pathogen state information usually correlates more closely with conventional microbiological assays based on growth in culture, which in turn relates more closely to infectious potential and relative health risks. However, if enough dead bacteria are present, endotoxins such as lipopolysaccharide can still pose a significant risk factor to human health. For this reason, it is important to try to obtain not only a relative number of live/dead bacteria but also a measure of total number.

It is also easier to quantify the absolute number of pathogens in different pathogen states using a multicolor fluorescence approach. The combination of SPR and molecular imaging also provides powerful proof that each measurement is a true-positive, rather than false-positive leading to greater detection accuracy. This imaging need not optically resolve individual pathogens. Relative numbers can be determined by total fluorescence measured, which gives an absolute number of pathogens within the variability of fluorescence staining of individual pathogens.

This device integrates an SPR imaging system with an epi-fluorescence molecular imaging system, both to determine what fraction of pathogenic bacteria are live or dead and to confirm the SPR results (23). A microfluidic chip encloses a biosensor array that will capture the sample. The array is functionalized with ligands specific to the pathogens that are to be detected.

Importance of "Preconcentrating" the Pathogens for Subsequent Analysis in the Device

Since microfluidic devices by definition can only sample small amounts of fluid, it is important and necessary to preconcentrate all possible pathogens present in large volumes of fluid prior to microfluidic analysis. Use of specific antibodies or other capture molecules, such as peptides or aptamers, works well but requires specific reagents and creation of a multiplexed magnetic capture molecule system. These nanoparticle-labeled pathogens can be captured and held against a surface while excess fluid is discarded. This translates to very large improvements in sampling statistics. There remains a need to develop more general capture methods that can easily select a number of different pathogens simultaneously.

COLOR

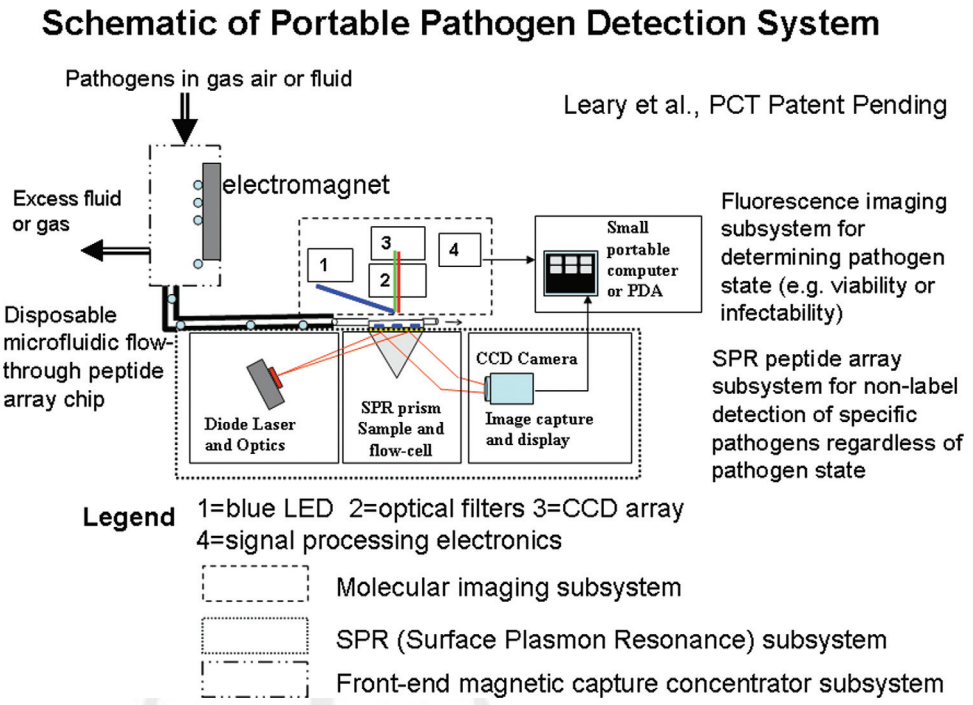

Figure 1. Multicomponent schematic of the overall pathogen detection system showing light paths and detection system. [Color figure can be viewed in the online issue, which is available at www.interscience.wiley.com.]

Materials and Methods

Overall Design of SPR Device

This hybrid, multicomponent device contains (1) a front-end magnetic concentrator to capture magnetic micro- or nanoparticle-labeled microbes and increase their concentration into a smaller volume suitable for a microfluidic flow/imaging device, (2) a surface plasmon imaging subsystem to detect captured microbes on a patterned grid of gold contact spots, (3) a molecular imaging epi-fluorescence subsystem to determine viability and functional status of the captured microbes, and (4) small imaging cameras to capture SPR and molecular imaging data coupled to a portable computing device (initially a laptop computer, but eventually a much smaller PDA-type device). This computing device can contain automated image analysis and other software to do completely automated analysis for pathogen detection. A schematic of the overall conceptual design of this portable foodborne pathogen detection system is shown in Figure 1.

Bacterial Strains, Growth, and Staining

Two strains of *E. coli*, pathogenic *E. coli* O157:H7 (Castellani and Chalmers strain, ATCC, Manassas, VA), and the non-pathogenic *E. coli* DH5-α (provided by Arthur Aronson, PhD, Department of Biological Sciences, Purdue University, West Lafayette, IN) were used for proof-of-concept experiments. The bacteria were streaked onto an LB (Luria-Bertani) plate and incubated at 37°C overnight. Single isolated colonies were aseptically harvested from the LB plate and allowed to grow in culture tubes containing 10 mL of LB broth, in an agitating incubator set to 200 rpm overnight at 37°C. Bacterial cultures were harvested when they reached an OD of 0.66 at 670 nm for the live DH5-α and 0.467 for the live O157:H7 bacteria.

To make sure that our growth conditions for our bacterial strains were optimized and to ensure that we had viable bacteria for our experiments, we performed a simple fluorescence method for live/dead bacteria determinations. *Bac*Light™ Bacterial Viability Kits (Invitrogen, Carlsbad, CA) provides a sensitive, single-step, fluorescence-based assay for bacterial cell viability employing two nucleic acid stains—the green-fluorescent SYTO®9 stain and the red-fluorescent propidium iodide (PI) stain (19–21,24). When used alone, the SYTO®9 stain labels both live and dead bacteria. In contrast, PI penetrates only bacteria with damaged membranes, reducing SYTO®9 fluorescence when both dyes are present. This assay is not a universal viability indicator for all species of bacteria, because it has been found that in multiple bacterial species will uptake PI during the exponential growth stage resulting in a false dead signal (24). Therefore, the efficacy of *Bac*Light™ kit must be verified for the desired pathogen strain. When the assay is applicable for the pathogen species, it is desirable to use because it can be completed in minutes and does not require wash steps. This assay was demonstrated to successfully discriminate between live and dead *E. coli* O157:H7 cells (see Supp. Info. Fig. S1). For this assay and all subsequent binding experiments, *E. coli* O157:H7 bacteria were incubated with 7.16 μM SYTO-9 and 17.14 μM PI for 10 min at room temperature per manufacturer's protocol.

Magnetic Preconcentration of Bacterial Sample

Magnetic preconcentration was accomplished using superparamagnetic carboxyl-functionalized Biomag® 1.5 μm iron oxide beads (Bang's Labs, Fishers, IN) coupled with antibodies specific to a membrane antigen on *E. coli* O157:H7 and then incubated with the *E. coli* O157:H7 (shown in Supp. Info.

Fig. S2). The method used to concentrate bacteria, as described in the "Results" section, involves use of a specific antibody against the bacterial strain that is being screened. This linked the bacteria to one or two magnetic beads. After washing with water, the coupled beads and bacteria were diluted with water into different concentrations from 1:10 to 1:100 with a total volume of 0.5 mL. Each sample was vortexed to create homogeneity immediately before the spectrophotometer reading was taken in a UV–vis spectrophotometer (Genesys 10uv, Thermo-Fisher, Waltham, MA) at 350 nm, which is a wavelength absorbed by iron oxide. Next, a 200 mT magnet was used to draw the magnetic beads to the side of the tube so that the supernatant fluid could be removed. An equivalent amount of water was then added to the beads and shaken. The absorbance at 350 nm of the resuspended bead mixture was then measured in the spectrometer. The supernatant fluid was also measured in the spectrophotometer to check for stray magnetic beads to help determine the capture efficiency. Atomic force microscopy imaging was performed to determine that 1–4 magnetic beads were bound to each *E. coli* cell (see Supp. Info. Fig. S3).

Microfluidic Chip Assembly

The microfluidic chip was manufactured using conventional soft lithography techniques. First, the chip was designed using Ansoft HFSS v10.1 software (Ansoft, Pittsburgh, PA). The design was tailored to create a sheet of fluid across a wide channel that would remain close to the gold surface to allow for maximum capturing capabilities. The resin mold (Accura SI 10 polymer, 3D Systems, Rock Hill, SC) for this chip was then created using a stereolithography machine (VIPER si2T SLA System by 3D Systems). Stereolithography was used because it could easily create a multidimensional shape with one mold as compared with photolithography that would have required several layers to achieve the height differentials needed to link the tubing (400 μm) to the flat chip (50 μm). Once the mold was cured with UV light, a 1:10 ratio of curing agent to polydimethylsiloxane (PDMS) polymer was mixed and then poured over the mold. This was allowed to cure overnight so that the pattern of the mold would be embedded onto the PDMS. Next, the PDMS was peeled off the resin mold, yielding microchannels for flow, and an inlet sample port was punched into the PDMS using a blunt-tipped 28-gauge needle. The PDMS was then placed onto a clean glass microscope slide (microchannel face down) and oxidized using a Corona plasma etch system (BD 20AC, Electro-Technic Products, Chicago, IL). The Corona system is a handheld device that creates a localized plasma field at room temperature. This was used to first oxidize the PDMS for ~20 s, and then the PDMS was pressed onto the glass slide and heated on a hotplate at 70°C for 15 min to ensure a good seal. The Corona process is important because it does not require higher temperatures that may damage antibodies, peptides, or other capture molecules during the process of bonding the microfluidic structure to the gold contact-printed slide. After the PDMS chip preparation, tubing was inserted into the port created by the blunt needle and sealed with liquid, uncured PDMS. The overall microfluidic chip assembly is shown in Figure 2. F2

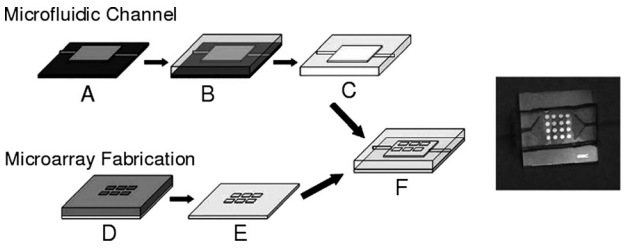

Figure 2. Schematic of the overall microfluidic chip assembly process showing the steps from the patterns of the microfluidic channels and grid to the finished SF10 glass chip: (**A**) SU-8 photoresist is patterned to make a silicon mold; (**B**) PDMS is poured on silicon mold and allowed to set; (**C**) PDMS replica with microchannels, (**D**) photolithography on SF10 glass chip; (**E**) gold evaporation and lift off; (**F**) PDMS chip is bound over the gold spot array using a Corona etcher. The constructed microfluidic chip (right).

Specific Pathogen Capture Process

The base chip used was a glass slide with a 4 × 4 array of 1-mm diameter gold spots (GWC Technologies, Madison, WI). Three biomolecules were used to functionalize the gold spots. The first was an antibody that specifically binds *E. coli* O157:H7. The second was rabbit preimmune serum as a negative control while the third was 0.5% bovine serum albumin solution in water (BSA Fraction V, Sigma-Aldrich, St. Louis, MO) as a second negative control. The array was patterned by applying 1 μL (at a concentration of 100 μg/mL) of a specific biomolecule to each gold spot, which was left to adsorb to the surface for 1 hour at room temperature. The chip was then washed with phosphate-buffered saline (PBS), followed by 0.5% BSA to occupy any remaining active sites on the gold surface, as well as nonspecific sites on the antibodies. Two strains of *E. coli*, *E. coli* O157:H7 and *E. coli* DH5-α, were then selectively introduced to the array by pipetting 1 μL of one of the bacteria suspension onto each spot after being fluorescently labeled with 7.16 μM SYTO-9 and 17.14 μM PI (Invitrogen). A hemacytometer was used to determine the concentrations of the bacteria, there was 3 × 106 cells/mL of *E. coli* O157:H7 and 2 × 108 cells/mL of *E. coli* DH5-α. The bacteria were allowed to incubate at room temperature for 10 min, and unbound bacteria were washed away with PBS.

Construction of Optical Components of SPR Imaging Subsystem

Our bench-top SPR imaging system was built on an optical breadboard using postmount optics, based on the Kretschmann configuration (24), whereby a thin gold film is directly deposited on a slide placed on top of a SFL11 equilateral prism (Edmund Optics, Barrington, NJ) that is used to generate the necessary evanescent wave at the metal-dielectric interface by means of total internal reflection, as described earlier. An inexpensive 635-nm diode laser (Edmund Optics) was placed on top of a SFL11 equilateral prism (Edmund Optics) and used to illuminate the sample. The prism is subsequently mounted on a

J_ID: Z3W Customer A_ID: 08-167 Cadmus Art: CYTO20692 Date: 23-NOVEMBER-08 Stage: I Page: 5

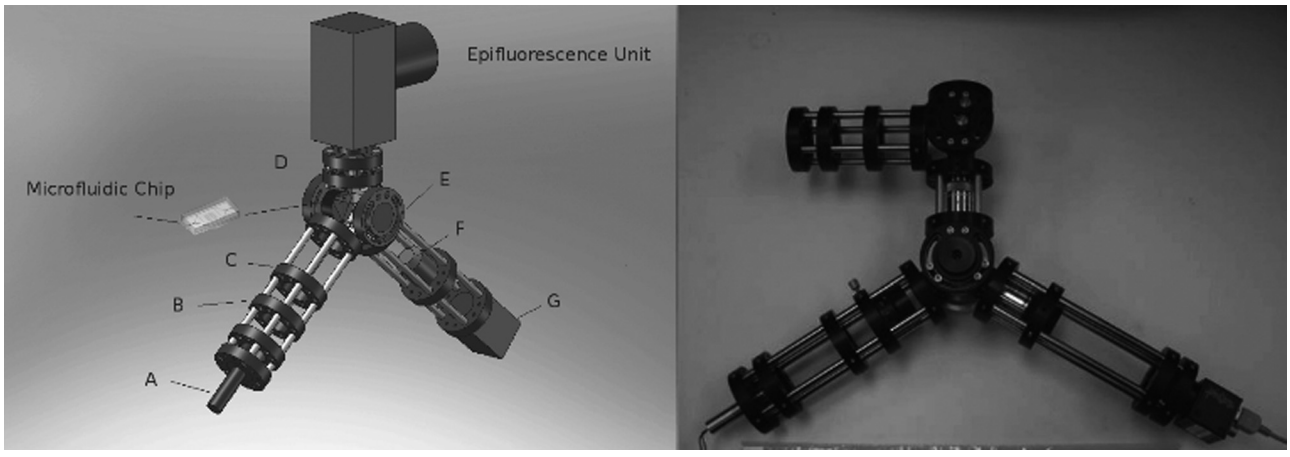

Figure 3. A schematic drawing of the next generation portable SPR imaging hybrid imaging system with associated microfluidic chip (left). The components of the SPR system consists of a 635-nm laser diode (**A**), a beam expander (**B**), a polarizer (**C**), a prism (**D**), continuous angle mounting plate (**E**), 4× objective (**F**), and a CCD camera. The microfluidic chip is inserted on top of the prism, and molecular imaging is performed from the top side of the chip using an LED illuminated epifluorescence unit. A picture of the constructed portable SPR imaging hybrid imaging system (right). The mini-optical rail system gives flexibility and structural integrity to the device so that it can be self-supporting and portable.

goniometer (Thorlabs, Newton, NJ), which is used to control the incidence angle of the laser. An inexpensive computer-controlled charge coupled device (CCD) camera (Pt. Gray Research, Richmond, BC, Canada) is then used to collect the SPR image.

Fluorescence Imaging of Bacteria

For this article, the capture of fluorescently labeled bacteria was assessed using epi-fluorescence microscopy (Nikon Diaphot Inverted Fluorescence Microscope; Nikon, Melville, NY). A fluorescence image of each spot was captured for both SYTO-9 (475/20 nm BPD excitation, 500 nm LPD, and 525/15 nm BPD emission filters were used; Omega Optics, Austin, TX) and PI (475/20 nm BPD excitation, 500 nm LPD, and 585/30 nm BPD filters; Omega Optics), and the presence of captured pathogen was quantified by using NIH ImageJ analysis software (http://rsbweb.nih.gov/ij/). The amount of captured bacteria was calculated from the SYTO-9 images for each spot. The images were first thresholded, using a threshold pixel value of 48 (8-bit image), which was 10% above the background intensity. Then the "Analyze Particles" function of ImageJ was used to determine the number of bacteria on each spot. Viability of the bacteria was determined using the PI images. The same ImageJ procedure was used to quantify the amount of PI-positive dead cells, except that the threshold used was a pixel value of 30, because a control sample of SYTO-9 only showed a fluorescent signal maximum of 25 with the PI imaging settings.

Design and Construction of the Portable Hybrid Imaging System

A more portable prototype of the hybrid imaging system has been subsequently designed and is shown in Figure 3. This prototype utilizes the Microptic optical cage system (AF Optical, Fremont, CA) to make a three-armed device. The SPR arms are also based on the Kretschmann configuration. This SPR imaging setup captures data for the entire probe array, including controls to detect nonspecific binding as described later in this proposal, simultaneously on a CCD camera. A BK7 glass right angle prism (Thorlabs, Newton, NJ) is mounted at the center of the three arms. The prism mounts contain variable angle slots, which allow the SPR illumination arm and detection arm, to swing to create the appropriate incident angle. The first SPR imaging arm, the illumination arm, consists of a 635-nm diode laser (Thorlabs) that is then shaped by a beam expander to illuminate the whole sample. A polarizer on a rotary mount (AF Optical) is used to generate p-polarized light. The SPR detection arm consists of a 4× long working distance objective (Olympus, Nashua, NH), a focusing lens, and a CCD camera (Pt. Gray Research) to capture the SPR image, whereas the epi-fluorescence imaging arm uses a 4× objective to image the sample, with the standard excitation (480/20 nm band pass) dichroic (500 nm long pass dichroic) and emission filter setup (515/20 or 565/30 nm band pass). An ultra-bright 470 nm LED is used to illuminate the sample (LumiLEDs, San Jose, CA) for molecular imaging of the fluorescently stained bacteria, and a monochromatic CCD camera (Pt. Gray Research) is used to image the sample. Both cameras are connected to a notebook computer (Dell Inspiron 1300, Dell Computers, Round Rock, TX) where frame grabber software acquires the images (PixelScope Pro, Wells Research, Lincoln, MA). The microfluidic chip was placed on top of the prism where it can be imaged by both SPR imaging and epi-fluorescence molecular imaging.

Results

Immunomagnetic Preconcentration and Capture Efficiency

E. coli O157:H7 cells were preconcentrated with magnetic beads in final 0.5 mL volumes and the efficiency of capture determined using ferric oxide absorbance measurements from

ID: kumaris Date: 23/11/08 Time: 15:54 Path: J:/Production/CYTO/Vol00000/080196/3B2/C2CYTO080196

Table 1. The recovery of magnetic bead-E. coli complexes measured by spectrophotometry at 350 nm

INITIAL DILUTION	INITIAL $A^{350\ nm}$	$A^{350\ nm}$ AFTER MAGNETIC RECOVERY	PERCENTAGE RECOVERY (%)
1:10	0.600A	0.547A	91
1:20	0.199A	0.185A	93
1:50	0.105A	0.097A	92.4
1:100	0.065A	0.062A	95

A spectrophotometer was used to measure the absorbance at 350 nm of several dilutions (1 mL volume) magnetic bead bound to *E. coli* complexes. After an initial absorbance at 350 nm was measured, a magnet was used to concentrate the complexes against the side of the tube, and then the supernatant was removed. The samples were then resuspended in 1 mL of distilled water and the absorbance was measured again. Using Beer's law, the percent recovery of the magnetic bead-*E. coli* complexes was greater than 90%.

a spectrophotometer as described previously. To demonstrate the physical capture ability of bound bacterial cells, as well as decrease the overall sample volume, the magnetic beads were exposed to a magnetic field that forced them to the side of the sample tube allowing for the removal of the supernatant (containing unbound bacteria as determined by microscopy). For all concentrations tested, there was greater than 90% recovery as shown in Table 1. The remaining 10% of the beads were likely lost during the wash and resuspension steps. There was no indication of magnetic beads left in the supernatant fluid based on spectrophotometer readings (data not shown). A small volume of the purified sample was observed under the microscope. The fluorescence of the stained bacteria indicated a successful linkage since the beads do not fluoresce (see Supp. Info.).

Specific Capture of *E. coli* O157:H7 on Biochip

The biochip was patterned with one of three biomolecules on each gold spot. The spots were either functionalized with an *E. coli* O157:H7 antibody or with one of the negative controls: rabbit preimmune serum or 1% BSA (Fraction V, Sigma Chemical, St. Louis, MO) as shown in Figure 4. This diagram also shows which spots were exposed to *E. coli* O157:H7 and which ones were exposed to the negative control strain of *E. coli* DH5-α. To demonstrate specific capture of *E. coli* O157:H7, bacteria should only be present on the gold spots functionalized with *E. coli* O157:H7 antibodies that were exposed to *E. coli* O157:H7. A fluorescence image demonstrating the binding of bacteria to the array is shown in the top right pane of Figure 4. It is clear that the spots with the highest intensity are those functionalized with *E. coli* O157:H7 antibodies and were exposed to *E. coli* O157:H7.

The binding of pathogens to each spot was quantified by image analysis using NIH ImageJ software. The results of this analysis are shown in Figure 5. The only conditions where a significant amount of coverage occurred were on gold spots

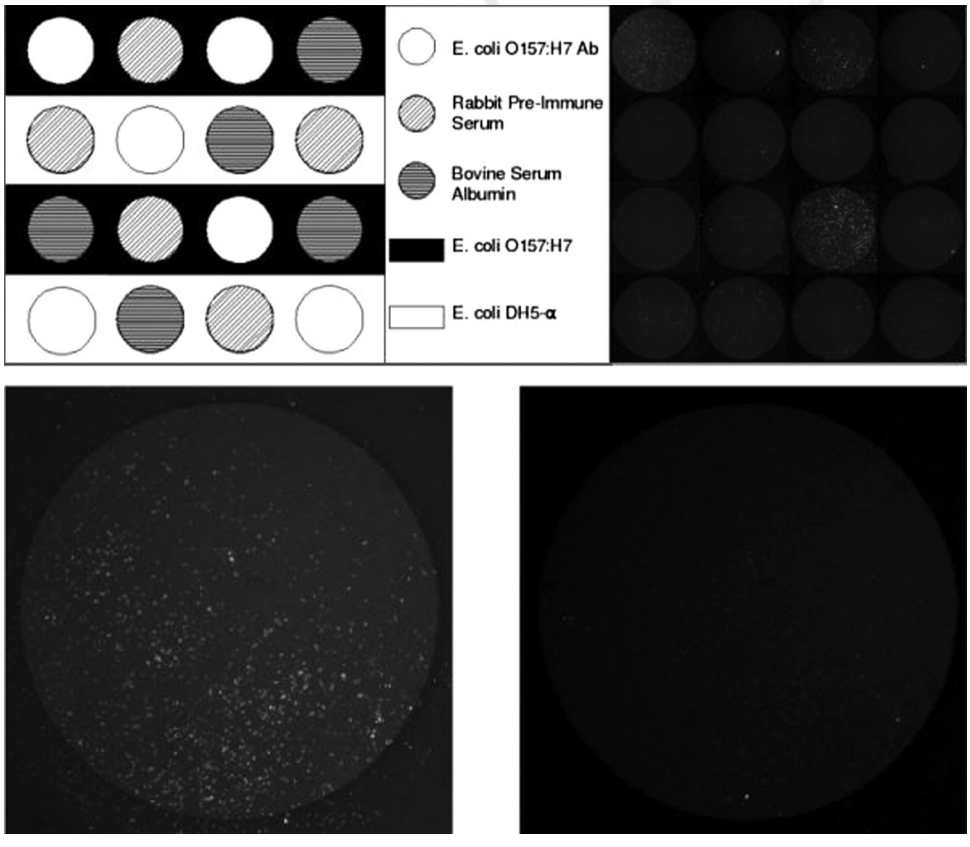

Figure 4. Top left: The pattern of functionalization of the gold array. Gold spots were functionalized with either *E. coli* O157:H7 antibody, rabbit preimmune serum, or 1% BSA. Then either *E. coli* O157:H7 (black background) or *E. coli* DH5-α (white background) were added to each spot. Top right: A fluorescence image of the gold array demonstrating the selective capture of pathogens. Bottom: Fluorescent images of one spot (row 1, column 3) showing the SYTO-9 signal (left) that shows how many cells are bound, and the PI signal (right) that shows the level of dead cells. The captured *E. coli* O157:H7 was bound to be 97.7% viable.

J_ID: Z3W Customer A_ID: 08-167 Cadmus Art: CYTO20692 Date: 23-NOVEMBER-08 Stage: I Page: 7

functionalized with *E. coli* O157:H7 antibodies that were exposed to *E. coli* O157:H7, where the mean number of bound bacteria to each spot was 1,653, and in the other cases, the mean number of bound bacteria was less than 300 cells. There was very little binding of *E. coli* O157:H7 to spots functionalized with rabbit preimmune serum or BSA, this demonstrates that there is only a little amount of nonspecific binding of *E. coli* O157:H7. As expected, the *E. coli* DH5-α showed low levels of capture regardless of the surface functionalization. The viability of the captured bacteria was measured by comparing the number of PI-positive bacteria to the total number of bacteria as determined by SYTO-9; the images are shown in the bottom row of Figure 4. The viability of *E. coli* O157:H7 specifically captured by the chip was found to be 97.7%.

Comparison of SPR Imaging and Fluorescence Imaging of Captured *E. coli* O157:H7

Examples of SPR images with corresponding fluorescence images on samples of different *E. coli* densities are shown in Figure 6. The SPR images and fluorescence images are not of the same field of view. Single pathogenic *E. coli* O157:H7 were successfully imaged using SPR and fluorescence imaging. Even if the fields of view were the same, SPR images only show the points where the bacteria are in contact (within SPR distance and conditions) with the gold surface. Hence, SPR images will only partially correlate with the fluorescence images because the latter represents a top view of all bacteria, whether or not they are within SPR imaging distance/conditions of the surface.

F6

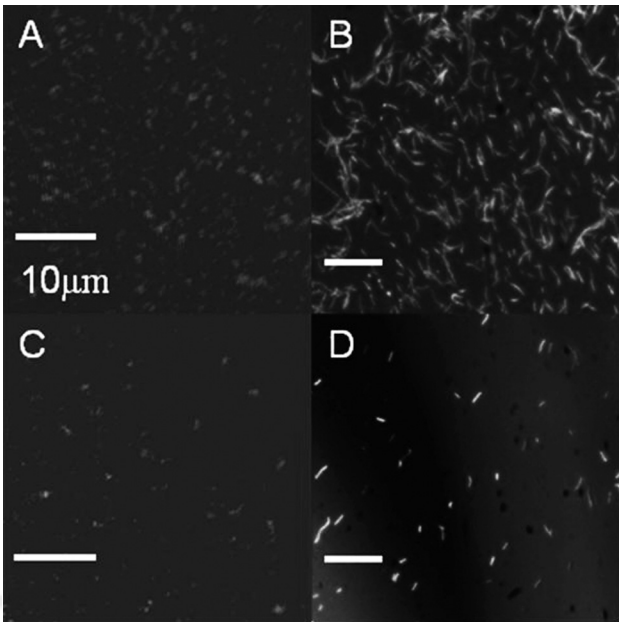

Figure 6. SPR images (**A** and **C**) and fluorescence images (**B** and **D**) of *E. coli* O157:H7 at high and low cell densities. Panels A and B were imaged from different areas on the same chip with a high cell density. Panels C and D were imaged from different areas of a second chip with a lower cell density.

Discussion

In this article, we have described the evolving design and current status of a foodborne pathogen testing device using *E. coli* O157:H7 as our pathogen of interest. The multicomponent design has permitted the parallel development of several interrelated subsystems as described earlier. The feasibility of the approach used for each subsystem is described and presented in terms of the data obtained. The design is evolving from an initial prototype mounted on an optical bench to a more portable "micro-optics" design, which is light-weight and potentially capable of being taken into the food production or preparation area for real-time testing for the multiplexed detection of foodborne pathogens.

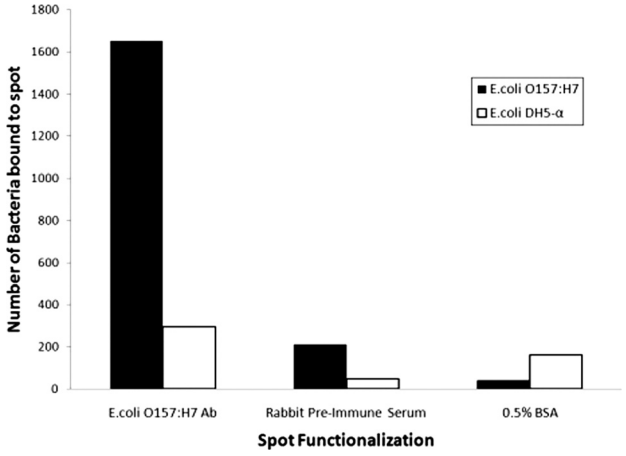

Figure 5. The number of bacteria bound to each spot depending on the strain of *E. coli* and the surface functionalization.

The hybrid imaging approach detection of pathogenic bacteria and an estimate of its relative infectivity through viability measures by fluorescence imaging in a portable device would represent a much needed advance in the testing of potential foodborne pathogens, introduced either accidentally or deliberatively into the food supply. The use of preconcentrating techniques with magnetic capture particles provides a more realistic way of sampling and concentrating larger volumes making a microfluidic approach feasible with sufficient sampling statistics to be meaningful. In the near future, we are looking to use this system to image a biosensor array to perform multiplexed pathogen detection. Using the 4 × 4 gold spot array chip affords the option of incorporating up to 16 different surface functionalizations on one chip. This will allow the simultaneous screening of up to 14 pathogen strains along with positive and negative controls. The system can image all 16 spot by SPR imaging, and the special localization of capture molecules on the array is known. This portable cytometry device would offer a great commercial advantage to the food processing industry since it is a portable device that provides label-free screening in the field without needing the time-consuming process of growing the sample in culture.

Acknowledgments

The authors acknowledge the support of the cleanroom facilities of the Birck Nanotechnology Center within Discovery

ID: kumaris Date: 23/11/08 Time: 15:54 Path: J:/Production/CYTO/Vol00000/080196/3B2/C2CYTO080196

Park at Purdue University for mask design of microchip. They gratefully acknowledge the advice and review of our atomic force microscopy data by Dr. Helen McNally at Purdue University, who is an expert in the field. This article was presented at a meeting in Bad Schandau, Germany, on May 22–25, 2008 organized by the EFB European Federation of Biotechnology, Section on Microbial Physiology.

Literature Cited

1. Deisingh AK, Thompson M. Detection of infectious and toxigenic bacteria. Analyst 2002;127:567–581.
2. Bohaychuk VM, Gensler GE, King RK, Wu JT, McMullen LM. Evaluation of detection methods for screening meat and poultry products for the presence of foodborne pathogens. J Food Prot 2005;68:2637–2647.
3. Hahm BK, Bhunia AK. Effect of environmental stresses on antibody-based detection of *Escherichia coli* O157:H7, *Salmonella enterica* serotype Enteritidis and *Listeria monocytogenes*. J Appl Microbiol 2006;100:1017–1027.
4. Hong BX, Jiang LF, Hu YS, Fang DY, Guo HY. Application of oligonucleotide array technology for the rapid detection of pathogenic bacteria of foodborne infections. J Microbiol Methods 2004;58:403–411.
5. D'Haese E, Nelis HJ, Uyttendaele M, Debevere J. Real-time detection of pathogenic bacteria in foods. In: B. Blais B, editor. Current Challenges in Food Microbiology. 2003. pp 111–134.
6. Amagliani G, Brandi G, Omiccioli E, Casiere A, Bruce IJ, Magnani M. Direct detection of *Listeria monocytogenes* from milk by magnetic based DNA isolation and PCR. Food Microbiol 2004;21:597–603.
7. Duburcq X, Olivier C, Malingue F, Desmet R, Bouzidi A, Zhou F, Auriault C, Gras-Masse H, Melnyk O. Peptide-protein microarrays for the simultaneous detection of pathogen infections. Bioconjug Chem 2004;15:307–316.
8. Pan Q, Zhang X-L, Wu H-Y, He P-W, Wang F, Zhang M-S, Hu J-M, Xia B, Wu J. Aptamers that preferentially bind type IVB pili and inhibit human monocytic-cell invasion by *Salmonella enterica* Serovar Typhi. Antimicrob Agents Chemother 2005;49:4052–4060.
9. Dong Y, Wilkop T, Xu D, Wang Z, Cheng Q. Microchannel chips for the multiplexed analysis of human immunoglobulin G-antibody interactions by surface plasmon resonance imaging. Anal Bioanal Chem 2008;390:1575–1583.
10. Koubová V, Brynda E, Karasová L, Skvor J, Homola J, Dostálek J, Tobiska P, Rosický J. Detection of foodborne pathogens using surface plasmon resonance biosensors. Sens Actuators B: Chem 2001;74:100–105.
11. Nelson BP, Grimsrud TE, Liles MR, Goodman RM, Corn RM. Surface plasmon resonance imaging measurements of DNA and RNA hybridization adsorption onto DNA microarrays. Anal Chem 2001;73:1–7.
12. Oh BK, Lee W, Chun BS, Bae YM, Lee WH, Choi JW. The fabrication of protein chip based on surface plasmon resonance for detection of pathogens. Biosens Bioelectron 2005;20:1847–1850.
13. Shank-Retzlaff ML, Sligar SG. Analyte gradient-surface plasmon resonance: A one-step method for determining kinetic rates and macromolecular binding affinities. Anal Chem 2000;72:4212–4220.
14. Williams LM, Evans SD, Flynn TM, Marsh A, Knowles PF, Bushby RJ, Boden N. Kinetics of formation of single phospholipid bilayers on self-assembled monolayer supports, as monitored by surface plasmon resonance. Supramol Sci 1997;4:513–517.
15. Homola J, Dostálek J, Chen S, Rasooly A, Jiang S, Yee SS. Spectral surface plasmon resonance biosensor for detection of staphylococcal enterotoxin B in milk. Int J Food Microbiol 2002;75:61–69.
16. Taylor AD, Ladd J, Yu Q, Chen S, Homola J, Jiang S. Quantitative and simultaneous detection of four foodborne bacterial pathogens with a multi-channel SPR sensor. Biosens Bioelectron 2006;22:752–758.
17. Berger CEH, Beumer TAM, Kooyman RPH, Greve J. Surface plasmon resonance multisensing. Anal Chem 1998;70:703–706.
18. Rothenhausler B, Knoll W. Surface-plasmon microscopy. Nature 1988;332:615–617.
19. Berney M, Hammes F, Bosshard F, Weilenmann H-U, Egli T. Assessment and interpretation of bacterial viability by using the LIVE/DEAD BacLight kit in combination with flow cytometry. Appl Environ Microbiol 2007;73:3283–3290.
20. Czechowska K, Johnson DR, van der Meer JR. Use of flow cytometric methods for single-cell analysis in environmental microbiology. Curr Opin Microbiol 2008;11:205–212.
21. Lahtinen SJ, Ouwehand AC, Reinikainen JP, Korpela JM, Sandholm J, Salminen SJ. Intrinsic properties of so-called dormant probiotic bacteria, determined by flow cytometric viability assays. Appl Environ Microbiol 2006;72:5132–5134.
22. Taghi-Kilani R, Gyürék LL, Millard PJ, Finch GR, Belosevic M. Nucleic acid stains as indicators of *Giardia muris* viability following cyst inactivation. Int J Parasitol 1996;26:637–646.
23. Leary JF, Park K, Acharya G, Aronson AI. Hybrid SPR/molecular imaging microfluidic device for detection of pathogens. US Patent60/983,412, 2007.
24. Shi L, Gunther S, Hubschmann T, Wick LY, Harms H, Muller S. Limits of propidium iodide as a cell viability indicator for environmental bacteria. Cytometry Part A 2007;71A:592–598.

AQ2

AQ1: Kindly provide department/division name (if any) for the affiliations 1 and 3.

AQ2: Kindly provide the publisher and the place of publication for Ref. 5.

AQ3: Author, if you want Figure 1 to be printed in color, please inform the editor when you return materials.